

# **Prototype Coil Evaluation for NSTX-U Replacement Inner Poloidal Field Coils**

Y. Zhai\*, C. Neumeyer, J. Dellas, N. Greenough, M. Kalish, J. Petrella, W. Que, S. Raftopoulos and the NSTX-U Coil Test Team

P.O. Box 451 Princeton Plasma Physics Laboratory, Princeton, NJ, USA

\*Phone: 609-243-3056, Email: yzhai@pppl.gov

*Abstract* – The National Spherical Torus eXperiment Upgrade (NSTX-U) is an innovative magnetic fusion device constructed at the Princeton Plasma Physics Laboratory (PPPL). In 2016, due to the failure of the PF-1a upper divertor coil which experienced a coolant blockage, the NSTX-U operation was suspended. A post-mortem investigation indicated that an undetected gradual deterioration of coil inductance preceded the coolant blockage leading up to the operational suspension. The project team decided that all inner PF upper and lower coil pairs, denoted PF-1a, PF-1b and PF-1c, shall be replaced with new coils of improved design and manufacture. The new prototype inner PF coils from four suppliers across the globe were evaluated at PPPL following a Prototype Technical Evaluation Procedure (PTEP). Mechanical inspection and electrical testing was performed to qualify each supplier.

This paper discusses the details of the mechanical and electrical tests and measurements performed on the complete coils. The test results were used to assess quality of turn-to-turn and turn-to-ground insulations of the prototype coils. Two prototype coils were power tested at PPPL for five pulses to reach its rated current and maximum temperature following the completion of low power electrical testing. During pulses the conductors experience a near adiabatic temperature rise and hoop stress. Between pulses, cold water enters the inlet and a cooling wave propagates through the

coils as slugs of cold water heat up to the conductor temperature and then pass through the coil to the outlet. Results show that full power testing did not change coil electrical characteristics. Each prototype coil was then sectioned into two halves to permit examination of the internal insulation, conductor spacing and vacuum pressure impregnation (VPI) quality. The high voltage breakdown test of sectioned coils was performed to evaluate turn and ground insulation breakdown voltage. The estimate for the production coils is based largely on the experience learned from the prototype coil program. One production coil will be tested by Sep 2019.

**Keywords:** *NSTX-U, fusion magnets, Poloidal field coils, prototype, coil testing*

## I. INTRODUCTION

The National Spherical Torus eXperiment Upgrade (NSTX-U) is a Spherical Torus of pulsed magnetic confinement device with plasma of 1-5 seconds duration. The NSTX-U, built by Princeton Plasma Physics Laboratory (PPPL) and housed at PPPL, is an upgrade of the original NSTX device that operated successfully for more than 10 years [1-2]. NSTX-U implemented two major upgrades: a new central magnet assembly for a higher field and current, and the installation of a 2<sup>nd</sup> neutral beam line for more power and current drive flexibility. Figure 1 shows NSTX-U as the world leading Spherical Torus (ST) and the cross-sectional view of the inner PF coils in the polar region. A number of issues hindered the 10 week operations in FY 2016, and operations eventually ended due to an internal short in PF1aU coil [3]. It has since been decided to replace all three inner PF upper and lower coil pairs. The NSTX-U Recovery Project is the implementation of Extent of Condition Corrective Action Plan (CAP) [4] that will bring NSTX-U back on-line as a critical national user facility for fusion science research, and

restore the device and support infrastructure to a reliable operating state at scientifically relevant performance levels.

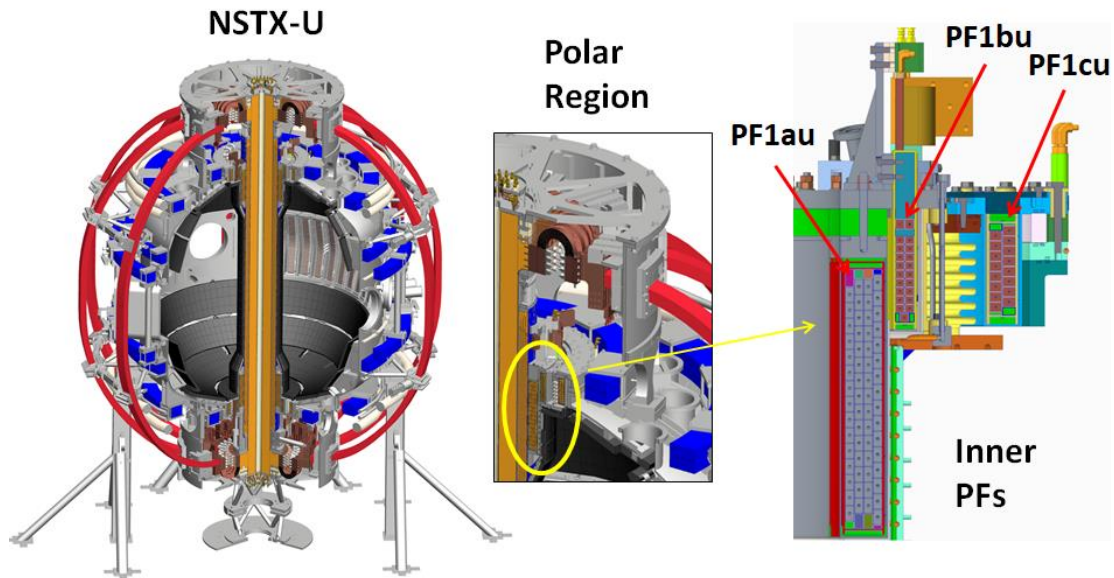


*Figure 1: NSTX-U is a Spherical Torus.*

Rebuilding all six inner-PF coils with a mandrel-free design for improved reliability is a major scope for the Recovery Project. The Inner PFs new mandrel-free design facilitates turn-to-turn electrical testing and improves coil manufacturability. For inner-PF coil ampacity,  $I^2t$  requirements that support program goals while reducing cool-down thermal stresses were redefined after several physics and engineering iterations [4-5]. The project team developed inner PF coil prototyping so vendors who would make production coils must first qualify by making a prototype coil, and having that coil go through a rigorous inspection and test procedure. The prototype coil technical evaluation process was comprised of the following steps for each prototype coil:

- Mechanical and electrical evaluation of the complete coil
- Power testing of the complete coil (two coils only)
- Sectioning of the prototype coil

- Mechanical and electrical evaluation of the sectioned coil

The project obtained prototype coils from four suppliers per a common specification [6]. Technical evaluation for the prototypes was completed in 3 months during the summer of 2018.

## II. PROTOTYPE TECHNICAL EVALUATION PROCEDURE

A high level summary of the testing methodology is shown in Figure 2 and selected evaluation results are described in [7-9]. The test methods are distilled from the process described in the Prototype Technical Evaluation Procedure (PTEP), which in turn calls out several specific procedures to implement the mechanical and electrical tests.

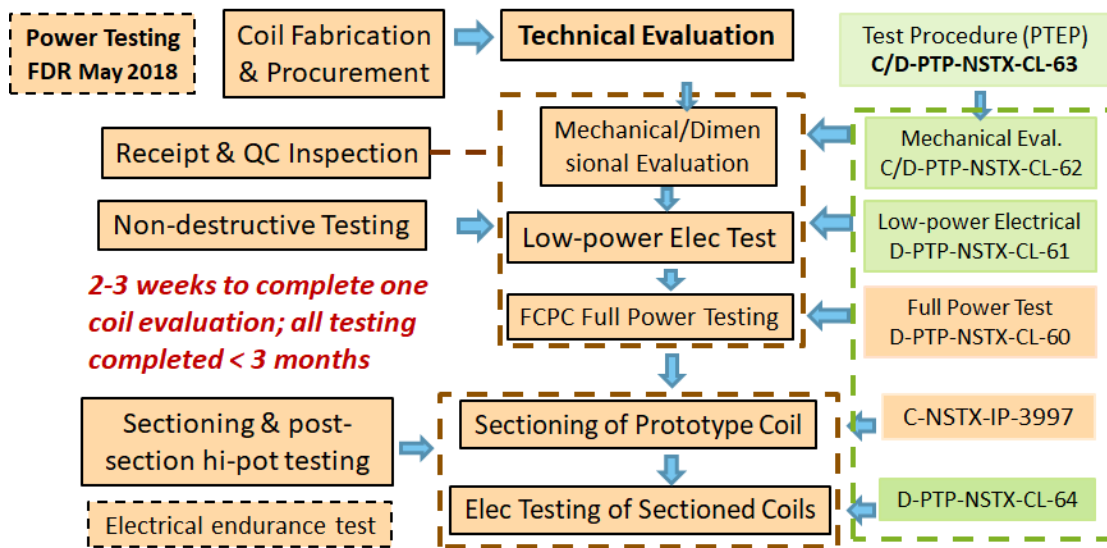


Figure 2: Overview of Inner PF Coil Evaluation.

### A. Inner PF Coil Description

The inner PF coils are water-cooled copper solenoids fabricated from rectangular shaped conductors with embedded central cooling channels. The coils, shown in Table 1, consist of three upper and lower pairs, denoted PF-1a, PF-1b and PF-1c and are energized up to 20 kA for about 1-2 seconds during plasma operations and then cooled

down with cold water once every 20 minutes. The coil turn insulation consists of two half-lapped layers co-wound woven glass fiber and Kapton tapes.

*Table 1 Inner PF Coil Dimensions and Design Parameters*

	Prototype	PF1a	PF1b	PF1c
Radius center conductor pack (mm)	324	325	392	556
Height of conductor pack (mm)	442	401	140	134
Conductor width x height (mm)	14x28	12x25	14x13	20x16
Number of turns	60	61	20	16
Number of layers	4	4	2	2
Cooling passage diameter (mm)	5.7	4.7	3.7	3.7
Pulse current (kA)	20.0	19.7	20.0	20.0
Equivalent square wave (sec)	3.1	1.9	1.0	1.4
Terminal-to-terminal voltage (kV)	2.0	2.0	2.0	2.0

### ***B. Mechanical Evaluation before Sectioning***

The non-destructive mechanical evaluation, including dimensional inspection of the complete coil, was performed per the purchasing specification [6] given to each coil supplier prior to shipping. An inspection report indicating all measured dimensions relative to their nominal per coil drawing was submitted to PPPL. PPPL performed a general inspection of workmanship and dimensions of the delivered prototype, complementing and validating the analysis done at the factory. Any noticeable defects and non-conformances were characterized and recorded. To ensure comparison validation of prototypes, test equipment and methodology used for all evaluations was identical for each coil including make, model, and serial number of test equipment [8-9].

**C. Low Power Electrical Test**

The electrical testing prior to sectioning consisted of basic electrical characterisation of low voltage measurements with nominal value expected shown in *Table 2*.

*Table 2 Low Power Electrical Characterization of the Prototype Coils.*

	Norminal	Equipment	Criteria
DC Resistance (mΩ)	5.8	Model DLRO10	20 °C temperature-corrected
Inductance (mH)	1.97	HIOKI IM3533-01	10 Hz reference frequency
AC Impedance (kΩ)		HIOKI L-C-R Meter	(10-2000) Hz, (1-200) kHz
Ground Wall Megger (GΩ)	>1	MIT 1020 Megger PE7043-W	500 V for one minute

The major impedance resonances of the prototype coil were located and quantified by the series and parallel resonance tests (with a 100 kΩ resistor inserted between the function generator output and the coil flags/oscilloscope) where the oscilloscope/probe and function generator were connected to the test coil terminal flags shown in Figure 3.

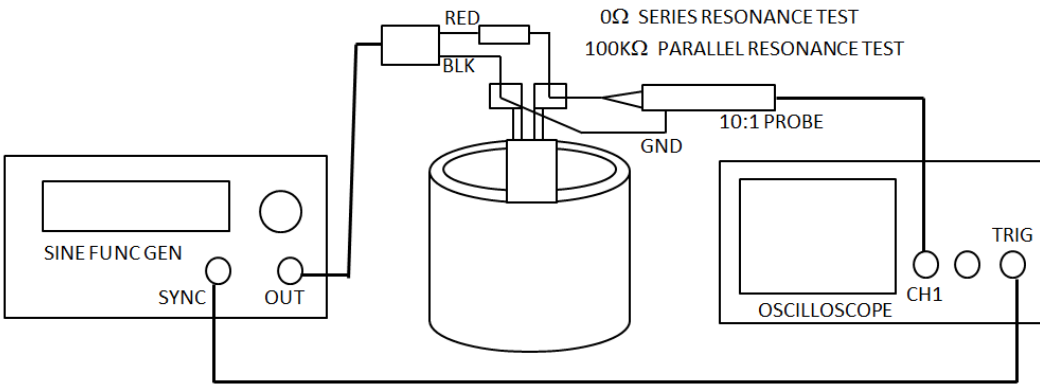


*Figure 3: Series and Parallel Resonance Tests.*

A specifically purchased and configured surge tester (Elytt CDG 7000) was utilized to confirm the dielectric strength of the coil’s turn-to-turn insulation. This system applied a short pulse of high voltage from a pre-charged capacitor, and measured the ringing LCR

response of the system. Electrical faults between the turns or the layers resulted in non-linear behavior in the waveform as the voltage was increased, or deviations in the waveforms between good and faulted coils [8].

#### **D. High Power Tests**

The first two coils received were power tested after completion of low power testing to ensure that at least one would successfully pass the end-to-end evaluation procedure. A series of current pulses were applied, increasing current and heating up to the rated current and maximum temperature. These pulses were designed to result in three equal increments of hoop stress ( $\propto I^2$ ) at short pulse, followed by three equal increments of total heating ( $\propto I^2 t$ ). The final pulse applied full field and heating. Examples of the pulse waveform and breakpoints are defined in Figure 4.

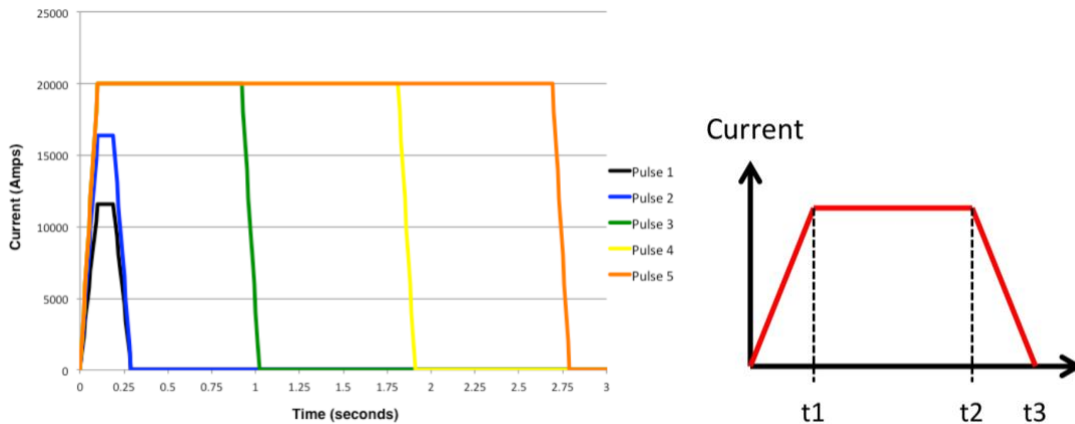


*Figure 4: Model pulse waveforms for power tests of the PF-1aP coil.*

#### **E. Mechanical Evaluation of Sectioned Coils**

Each of the prototype coils was cut into two sections for further inspection. The cuts were made 90 degree off from the coil leads as shown in Figure 5. Care was taken to ensure minimal surface damage, and a skimming cut (small depth, slow tool feed) was used to fully polish the surface.

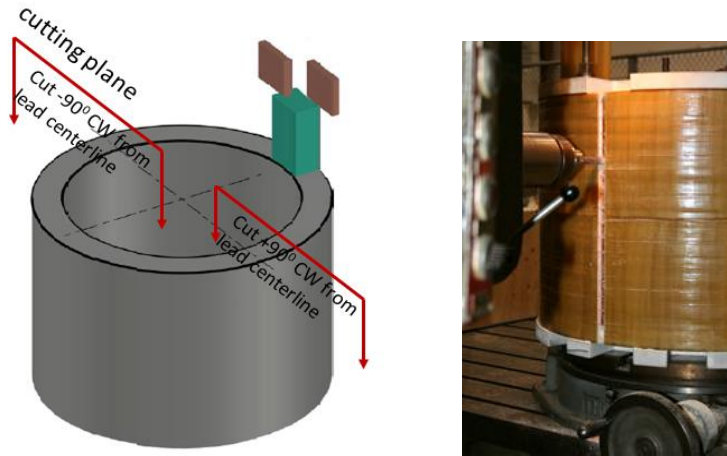


Figure 5: Sectioning of the prototype coil

After sectioning, the coil section ends were visually examined under magnification and the accuracy of the conductor positioning and insulation thickness within the winding pack array was measured. Any voids evident in the turn or ground insulation were noted including void size and location, cracks, crazing such as surface cracks, de-laminations, and dry spots within the insulation. Special attention was paid to the potential resin-rich areas during the examination. Surface examination was undertaken using magnification as necessary with photographs taken to aid further analysis of any potential defects. Logging flaws were compared among vendors to determine the quality of the prototype.

#### **F. Electrical Testing of Sectioned Coils**

After visual examination, the section ends were immersed in a dielectric fluid to increase the flashover voltage between the ends of cut turns for electrical evaluation.

Table 3: Insulation Electrical Strength Tests.

	Insulation	Acceptance Criteria
Megger	turn-to-turn	500V DC for one minute
DC breakdown	turn-to-turn	10 kV for one minute
	turn-to-ground	No breakdown at 20 kV

The breakdown tests shown in Table 3 confirm the ultimate capability of the electrical insulation system up to the level where flash-over at the end of the sectioned coil limits the applied voltage. For sectioned prototype coils with significant voids in the turn-to-turn insulation that possibly extended the entire circumference of the half-coil section (as evidenced when compressed air injected at one end section came out the other end), there was a concern when the sectioned coil was immersed in Fluorinert, the Fluorinert would enter the void region, improve its dielectric strength compared to air, and thereby artificially alter the insulation test results. It was decided to plug the section void ends at the sections to prevent ingress of Fluorinert. On each significant void and prior to immersion of the coil samples in Fluorinert, low pressure compressed nitrogen was injected, and vacuum cleaner applied to one or both ends to remove any flakes of copper that may have entered during the machining/sectioning process. Then, after cleaning the surfaces with alcohol, a small amount of RTV was applied to plug the open ends of the voids.

#### ***G. VPI Cured Resin Test***

A small piece of the cured epoxy sample post VPI process was obtained from each vendor to examine the quality of their VPI process. The material property measurements were performed via Differential Scanning Calorimetry (DSC) per ASTM E1356 to confirm the glass transition temperature ( $T_g$ ). The resultant  $T_g$  acceptance criteria was within a band of  $7\text{ }^{\circ}\text{C}$  of the target  $T_g$  (i.e., either that specified by the resin supplier or a benchmark value determined from lab samples that have undergone the same cure cycles as the coil in terms of times and temperatures). If a sample recorded a low  $T_g$  (outside benchmark value minus  $7\text{ }^{\circ}\text{C}$ ), the sample was post-cured and that

sample was re-measured. If  $T_g$  rose to the desired value, the sample was under-cured. If  $T_g$  failed to rise, it suggested an incorrect mix ratio.

### III. TEST RESULTS

#### A. Mechanical Inspection

Mechanical evaluation and dimensional inspection was performed on a granite table with a calibrated surface. A calibrated Romer Arm was used to take measurement points at 45 degree increments on the inside and outside surfaces, at heights corresponding to 1" increments from datum per coil drawing. A gauge block was used to measure the two smaller dimensions per coil drawing at the lead terminal flags. Figure 6 shows the four PF-1a prototype coils and Figure 7 and Figure 8 show the surface cracks evident on the outer surface of the coil. *Table 7* Results of dimensional inspection for all four prototype coils are summarized in *Table 4*. Inner radius and cylindricity are critical dimensional control parameters. All four prototype coils met the critical tolerance requirements although the outer radius and height were slightly off for one coil. This can be machined off to meet the critical tolerance requirements.

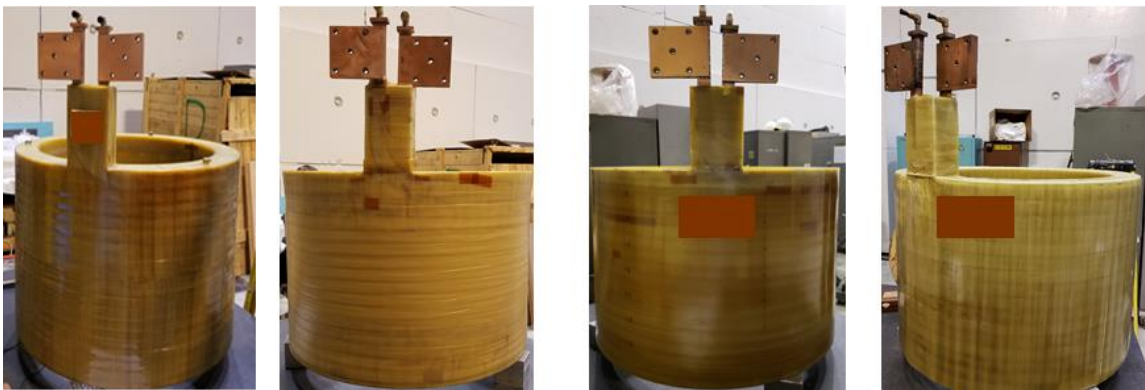


*Figure 6: The four PF-1a prototype coils as received by PPPL.*

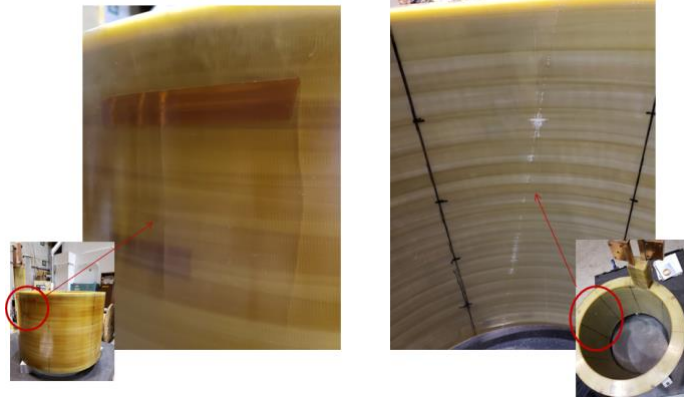


Figure 7: Surface cracks evident on outer surface of the prototype coil.

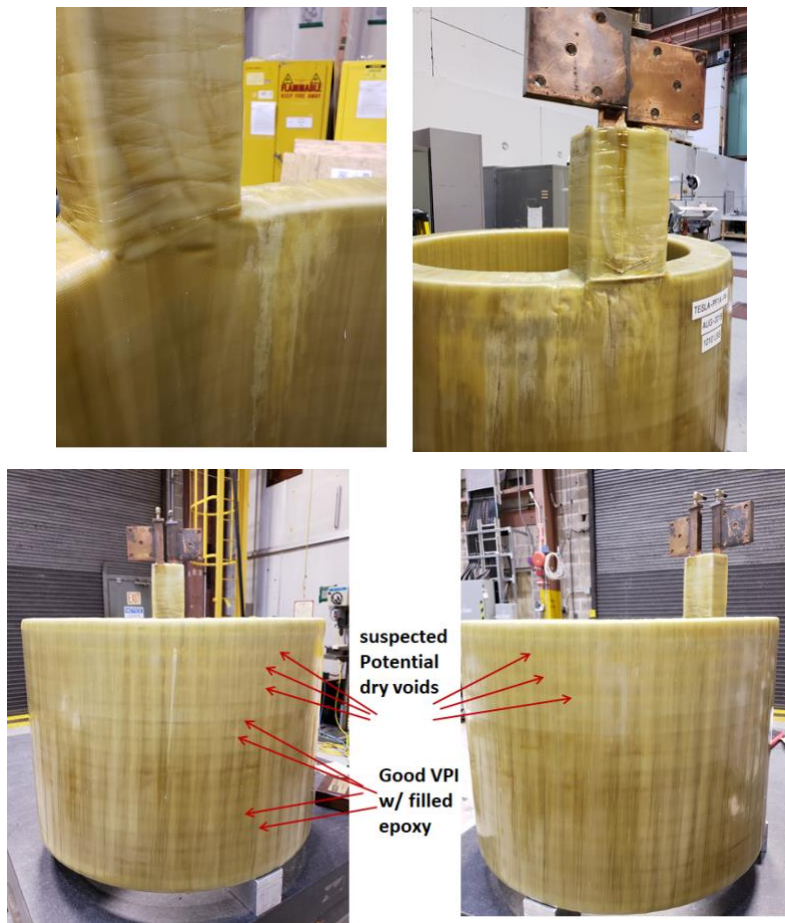


Figure 8: Some surface areas appear to be dry as indicated by color on outer surface of the prototype coil.

Table 4: Dimensions of prototype drawings and prototype coils.

		Nominal	Tolerance	Measured deviation	OK

		Inch	meter	Inch	mm	mm	
Inner Radius	Coil 2	11.311"	0.2873	0.03"	0.762	+0.5/-0.2	Yes
Outer Radius		14.211"	0.3610	0.05"	1.270	+1.2/-1.7	Yes
Height		19.74"	0.5014	0.06"	1.524	+0.2/-0.7	Yes
Inner Radius	Coil 1	11.311"	0.2873	0.03"	0.762	+0.3/-0.4	Yes
Outer Radius		14.211"	0.3610	0.05"	1.270	+1.5/-1.8	Yes
Height		19.74"	0.5014	0.06"	1.524	+2.5/-0.4	No
Inner Radius	Coil 3	11.311"	0.2873	0.03"	0.762	-0.1/-0.3	Yes
Outer Radius		14.211"	0.3610	0.05"	1.270	+0.4/-0.0	Yes
Height		19.74"	0.5014	0.06"	1.524	+0.2/-0.4	Yes
Inner Radius	Coil 4	11.311"	0.2873	0.03"	0.762	+0.0/-0.7	Yes
Outer Radius		14.211"	0.3610	0.05"	1.270	+2.0/-0.7	No
Height		19.74"	0.5014	0.06"	1.524	+1.1/-0.9	Yes

## **B. Electrical Evaluation**

The coil resistance (corrected to 20 °C) and inductance measured at PPPL are shown in Table 5. The values reported here were the averaged over three time measurements.

The Hioki IM3533-01 L-C-R meter was used to perform a low frequency AC impedance sweep from 10 Hz (~DC) to 2 kHz to cover the range of power supply rectifier harmonics, and 1 kHz to 200 kHz sweep to identify the resonance frequencies where equivalent capacitive impedance of the coil insulation matched the inductive impedance of coil winding. Series and parallel resonance measurements were performed using the test setup shown in Figure 3. The results are given in Table 5.

*Table 5: Coil Resistance, Inductance and Resonance Frequencies.*

	<b>Coil 1</b>	<b>Coil 2</b>	<b>Coil 3</b>	<b>Coil 4</b>
DC Resistance (mΩ)	5.67	5.66	5.67	5.70
Near DC Inductance (mH)	1.80	1.79	1.79	1.81
Parallel Resonance (kHz)	73.3	69.6	72.0	75.9
Series Resonance low-Q (kHz)	301	281	295	308
Series Resonance high-Q (kHz)	1058	1002	1050	1086

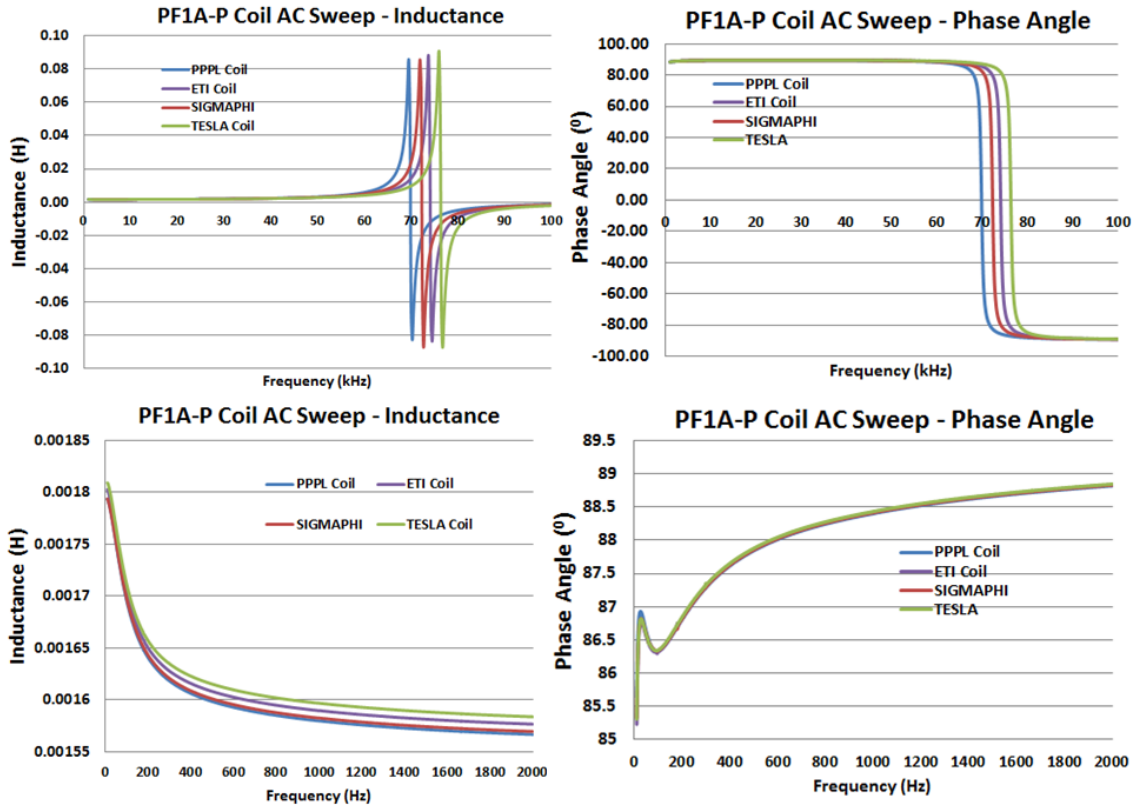


Figure 9: Impedance sweep for electrical characterization of all four prototype coils (comparison of results for all four coils tested at coil shop)

The impedance sweep shown in Figure 9 indicates about 10% difference of measured inductance between coil 2 and coil 4. This could be partially attributed to differences in the insulation thickness measured between the two coils as shown in Table 8.

The ground wall insulation resistance of each coil was measured at PPPL. A ground plane was formed using aluminum foil that was pressed against the ground wall using an inflated plastic membrane. *Insulation resistance measurements for both coils were all well above the 1 GΩ minimum requirement.* Typical results are given in [8].

Since turn-to-turn fault was the failure mode of the original PF1aU coil, turn-to-turn factory acceptance testing was a high priority and high visibility task. Surge test established during the prototype coil evaluation process will be used for turn-to-turn

factory acceptance testing. Acceptance is based on evaluation of response as follows: 1) comparison with theoretical value, 2) comparison at incremental test voltage levels, and 3) comparison between identical coils. Figure 10 presents the waveforms for 5 kV pulses for all prototype coils. All coils looked good with minor differences in ringing frequency after a few cycles, possibly due to small difference in coil inductance from coil geometry.

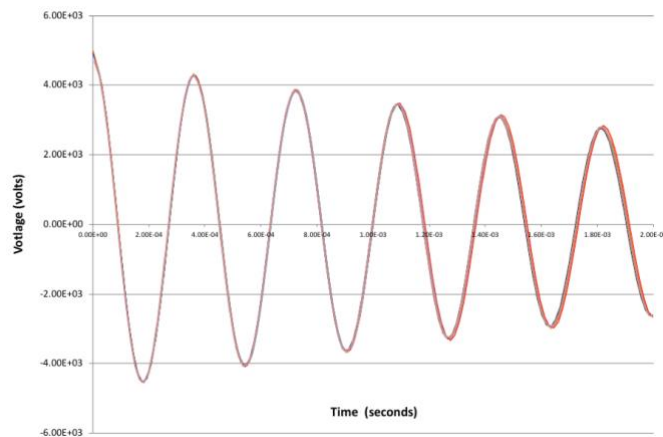


*Figure 10: Waveforms for 5 kV 1<sup>st</sup> and 10<sup>th</sup> pulses, all four prototype coils.*

### **C. Power Tests**

The Field Coil Power Conversion (FCPC) test facility dictated details of the coil test. Cooling water in the FCPC building was provided at a maximum of 25 °C whereas the NSTX Test Cell cooling water is 12 °C. Given the desire to limit the final temperature to one that the coil was qualified for and that production coils will experience in the field, the temperature rise during these tests was less than in service by  $25-12 = 13$  °C. To this end, sufficient joule heating was applied for the coil to reach the maximum temperature anticipated during full power operation. The actual waveforms shown in Figure 11 and set-points shown in Table 6 were adjusted based on operating conditions on the day of the test (water inlet temperature, power supply control precision).

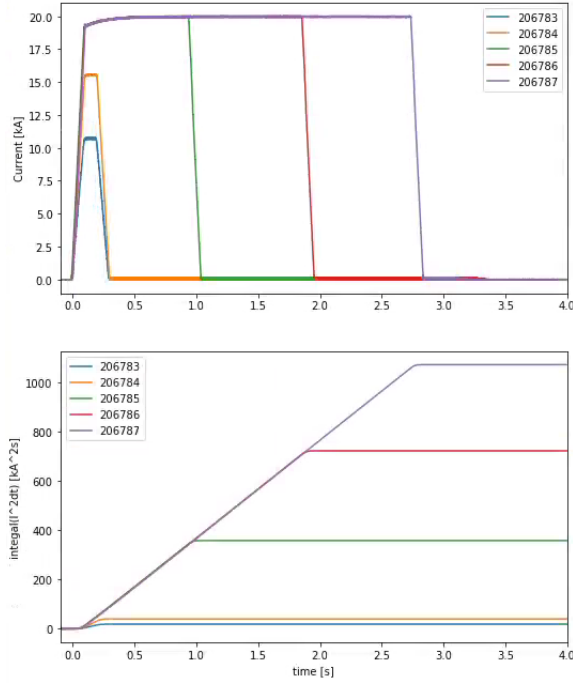


Figure 11: Actual current pulse waveforms (top) and Actual integral (bottom).

Table 6: Properties of target and achieved waveforms used on the PF-1aP coil.

Pulse	Target Flat-Top Current	Achieved Flat-Top Current	Target $\int I^2 dt$	Achieved $\int I^2 dt$
	kA	kA	kA <sup>2</sup> s	kA <sup>2</sup> s
1	11.547	11.547	22.2	22.2
2	16.330	16.330	44.4	44.4
3	20.000	20.000	365	365
4	20.000	20.000	729	729
5 (Coil 1)	20.000	20.000	1070	1070
5 (Coil 2)	20.000	20.000	986	986

#### D. Mechanical Evaluation of Sectioned Coil

Visual inspection of sectioned coil ends was performed under magnification and illumination for a comparison of manufacturing processes as shown in Figure 12. This included inspection of critical tolerances of conductors and insulation in winding pack. Voids evident in the turn or ground insulation were also noted as shown in Figure 13.



Figure 12: Sectioned prototype coils for a comparison of manufacturing process.

Continuous voids were found in Coil 1, along the toroidal channels proximal to turn corners at the sectioned ends. Non-continuous toroidal voids were found in each of the sectioned half of Coil 4, with void dimension shown in Table 7. Small, non-continuous voids were found in Coil 2. No voids evidenced in Coil 3.

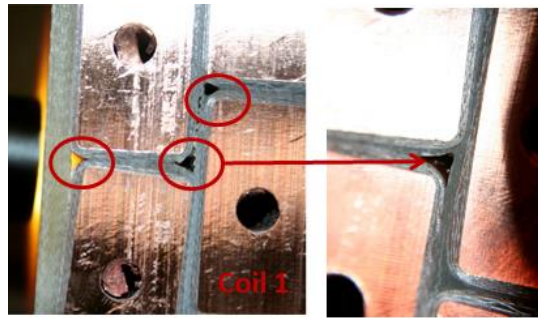


Figure 13: Toroidal voids found in sectioned coils

Table 7: Dimension of voids evidenced in sectioned prototype coils.

	Coil 4 – no-lead section				Coil 4 – lead section			
Labels	A	B	C	D	AA	BB	CC	DD
Diameter (“)	0.035	0.1	0.1	0.125	0.1	0.05	0.075	0.125
Depth (“)	0.25	0.16	1	1	0.5	0.8	1	n/a

Turn insulation layer transition different from the drawing was noted. For the production coil, the drawing was upgraded to add information and make transition locations clearer. PPPL will also provide greater vigilance to ensure transitions occur at predicted locations.

All sectioned coils show conductor turn twisting as result of conductor supplied to each vendor, which all exhibited different amounts of twisting. Inline hardening of conductor will reduce twist. For the production coil, we will focus on twist removal tooling within the MIT plan. Significantly reduced twist was achieved in production coil conductor as shown in Figure 14.



Sectioned Proto Coil 3



Figure 14: Turn twisting in sectioned prototype (left); production coil conductor (right)

Optical measurements of the insulation thickness were performed for all four prototype coils after sectioning. The measurements included turn-to-turn and turn-to-ground insulation thickness for each turn to quantify uncertainty on the variation of coil fabrication process. Table 8 is a comparison of nominal and minimum turn insulation thickness for four coils. The deviation could be due in part to conductor twist, and in part to excess compression of insulation during winding. Because of a very large safety factor (ratio of dielectric strength to applied voltage), the minimum thicknesses are acceptable. However, measurements should be taken during the manufacturing process to achieve dimensions that are closer to nominal.

Table 8: Turn-to-turn insulation thickness and range of thickness in sectioned coils.

	Coil 1	Coil 2	Coil 3	Coil 4
<b>nominal (")</b>	0.082	0.082	0.082	0.082
<b>minimum (")</b>	0.075	0.06	0.0675	0.0775
<b>Average (")</b>	0.087	0.084	0.083	0.087

range of variation (“)	0.045	0.0775	0.045	0.03
------------------------	-------	--------	-------	------

### **E. VPI Cured Resin Test**

The test results in Table 9 confirmed that the material was fully cured in the coils from all four suppliers. The slightly lower Tg from the coil 4 sample may simply be a reflection of where the sample was taken with regard to where the heaters were. It should not have any significant effect on the performance of the coil since the overall degree of cure in the system is in excess of 90% and, maximum mechanical properties will be realized at that stage. It may also be possible that the coil 4 sample did not get as hot as other places in the coil or that the overall temperature in the oven did not get as high.

*Table 9: DSC Data for CTD standard reference sample and the prototype coil resin*

Specimen #	Weight (mg)	$\Delta H$ (J/g)	Tg ( $^{\circ}C$ )	% Cure
CTD Standard	5.500	30.09	Not evaluated	96.58
CTD-425 Coil 1 Resin	9.80	37.37	178.87	95.76
CTD-425 Coil 2 Resin	10.4	36.25	171.63	95.88
CTD-425 Coil 3 Resin	8.6	45.83	176.05	94.79
CTD-425 Coil 4 Resin	6.5	56.70	164.02	93.56

## **IV. CONCLUSIONS & FUTURE WORK**

The NSTX-U Recovery Project, on track to enhance NSTX-U reliability and safety and to provide a high performance user facility, has obtained and evaluated all four prototype inner PF replacement coils supplied globally in summer 2018. All four coils successfully passed mechanical evaluation prior to sectioning. No external defects were noted, except that one coil had shallow cracks in resin-rich areas of the ground wall insulation, and dry spots were noted on the inner and outer surface of the other coil. Mechanical evaluation after sectioning revealed some imperfections as follows:

- Some voids were evident in turn-to-turn insulation in three coils.

- There was some variability in the turn-to-turn insulation thickness in three coils.

All four coils successfully passed all electrical tests, including high power testing of two prototype coils tested at both the maximum rated current and at maximum joule heating. Low power electrical tests repeated after high power tests showed no change in coil electrical properties, (Coil electrical insulation properties were unmodified). The four prototypes were successfully sectioned, visually examined, and fully cured resin material properties were confirmed for all four coils using a Differential Scanning Calorimetry (DSC) test.

#### REFERENCES

- [1] C. Neumeyer et al., "Engineering design of the National Spherical Torus Experiment," *Fusion Engineering and Design*, **54**, 275-319, (2001).
- [2] J. Menard et al., "Overview of the physics and engineering design of NSTX Upgrade," *Nuclear Fusion*, **57**, 10, June (2017).
- [3] J. Menard et al., "Overview of NSTX Upgrade initial results and modeling highlights," *Nuclear Fusion*, **57**, 10, June (2017).
- [4] S.P. Gerhardt et al., "Overview of the NSTX-U recovery project physics and engineering design," *IAEA FEC*, **26**, 8 (2018).
- [5] M. Kalish et al., "PF Coil Prototype Design Review," Final Design Review for Inner PF Prototype Coil at PPPL, June 7, 2017.
- [6] S. Raftopoulos, "Specification for Prototype – Phase 1 Inner PF Coils," NSTX-U-SPEC-MAG-004-R3, March, 2018.
- [7] Y. Zhai et al., "Design and Analysis of NSTX-U Inner PF Coils," SOFE, to be published (2019).

[8] C. Neumeyer et al., “Electrical Testing of NSTX-U Inner Poloidal Field Coils,” SOFE, to be published (2019).

[9] Y. Zhai et al., “Inner PF Coil Prototype Coil Notable Report,” PPPL report, NSTX-U-REC-039-00, July 12, 2018.

[10] Y. Zhai et al., “Inner PF Coil Prototype Coil Evaluation Report,” PPPL report, NSTX-U-REC-040-00, Sep 12, 2018.